(2) Nishi, T.; Wang, T. T. *Macromolecules* **1975**, *8*, 909
(3) Paul, D. R.; Altamirano, J. O. *Adv. Chem. Ser.* **1975**, *No. 142*, 371.
(4) Wendorff, J. H. *J. Polym. Sci., Polym. Lett. Ed.* **1980**, *18*, 445.
(5) Bernstein, R. E.; Cruz, C. A.; Paul, D. R.; Barlow, J. W. *Macromolecules* **1977**, *10*, 681.
(6) Hirata, Y.; Kotaka, T. *Polymer J.* **1981**, *13*, 273.
(7) Sasabe, H.; Saito, S.; Asahina, M.; Kakutani, H. *J. Polym. Sci., Part A-2* **1969**, *7*, 1405.
(8) Yano, S. *J. Polym. Sci., Part A-2* **1970**, *8*, 1057.
(9) Morra, B. S. Ph.D. Thesis, University of Massachusetts, Amherst, MA, 1980.
(10) Hermann, O. Master Thesis, Deutsches Kunststoff Institut, Darmstadt, FRG, 1984.
(11) Hahn, B. Ph.D. Thesis, Deutsches Kunststoff Institut, Darmstadt, FRG, 1983.
(12) Mikhailov, G. P.; Borisova, T. I.; Dmitrochenko, D. A. *Sov. Phys.-Tech. Phys. (Engl. Transl.)* **1956**, *26*, 1857.
(13) Monnerie, L., private communication.
(14) Popli, R.; Mandelkern, L. *Polymer Bull.* **1983**, *9*, 260.
(15) Popli, R.; Glotin, M.; Mandelkern, L.; Benson, R. S. *J. Polym. Sci., Polym. Phys. Ed.* **1984**, *22*, 407.
(16) Flory, P. J. *J. Am. Chem. Soc.* **1962**, *84*, 2857.
(17) Flory, P. J.; Yoon, D. Y.; Dill, K. *Macromolecules* **1984**, *17*, 862.
(18) Yoon, D. Y.; Flory, P. J. *Macromolecules* **1984**, *17*, 868.
(19) Görlitz, V. M.; Minke, R.; Trautvetter, W.; Weisgerber, G. *Angew. Makromol. Chem.* **1973**, *29/30*, 137.
(20) Yoon, D. Y.; Hahn, B., in preparation.
(21) Naegele, D.; Yoon, D. Y. *Appl. Phys. Lett.* **1978**, *32*, 132.
(22) Takahashi, N.; Odajima, A. *Jpn. J. Appl. Phys.* **1981**, *20*, L59.
(23) Furukawa, T.; Date, M.; Fukada, E. *J. Appl. Phys.* **1980**, *51*, 1135.

Interactions between Smooth Solid Surfaces in Solutions of Adsorbing and Nonadsorbing Polymers in Good Solvent Conditions

Paul F. Luckham† and Jacob Klein*‡

Cavendish Laboratory, Cambridge, England CB3 0HE. *Received July 11, 1984*

ABSTRACT: Direct measurements of the interaction forces $F(D)$ between two atomically smooth solid (mica) surfaces immersed in toluene have been carried out as a function of surface separation D; interaction profiles were also measured following introduction of (i) poly(ethylene oxide) (PEO) and (ii) polystyrene (PS) into the toluene (at low concentrations) and incubating the surfaces overnight in the solutions. Toluene is a good solvent for both polymers. In the pure toluene the interactions were short-ranged (≤10 nm) and attractive. Following full overnight adsorbance of PEO a quasi-equilibrium force–distance law was indicated on compression/decompression of the surfaces, with repulsion commencing at $D \simeq (8.5 \pm 1)R_g$ (unperturbed radii of gyration for the three molar mass polymers studied) and increasing monotonically at lower D. Rapid compression/decompression resulted in general in lower $F(D)$ values for a given D. This behavior qualitatively resembles that between adsorbed PEO layers in aqueous 0.1 M KNO_3 electrolyte, as reported earlier. In the PS/toluene solution, no adsorbance of polymer was indicated even after overnight incubation of the surfaces: the force–distance profiles were unchanged (within error) relative to those in the polymer-free solvent. A consideration of the magnitude of "depletion layer" forces suggests these (if any) would be undetectable at the polymer concentrations (10^{-4} (w/w)) used in our experiments.

Introduction

The technological exploitation of macromolecules to stabilize colloidal dispersions has a long history,[1] but it is only in the past few years that interactions between polymer-bearing surfaces, which are responsible for steric stabilization, have been studied directly.[2] Earlier measurements involved surface balance[3] and compression-cell techniques;[4] later, more direct determinations were made of the forces between two adsorbed polymer layers.[5,6] Recently, the "mica technique", developed by Tabor and co-workers,[7] and modified by Israelachvili and co-workers to study interactions between two mica surfaces immersed in a fluid,[8] has been extended by us to the case where the mica sheets bear polymer layers adsorbed from solution.[9-15] In addition to its directness and sensitivity, this method has the advantage of measuring attractive forces (if any) as well as repulsion between the adsorbed layers, which was not the case with earlier approaches.

Previous studies have included the case of polystyrene (PS) adsorbed onto the mica from cyclohexane, in poor solvent conditions:[9] the forces $F(D)$ between the two polymer-bearing mica surfaces a distance D apart were measured; the results showed a marked long-range attraction between the adsorbed layers ($F(D) < 0$), which was interpreted in terms of an osmotic attraction between the overlapping polymer layers. Later studies[12,14] in this system probed the effect of raising the temperature T to $T \geq \Theta$, the Flory Θ temperature; the forces between adsorbed layers in cyclopentane at $T \geq \Theta$ were also studied.[15] The interactions between adsorbed polyelectrolyte layers, poly(L-lysine), in aqueous KNO_3 solution were investigated[11] and showed thick, repulsive layers which were irreversibly compressed to yield a final short-range repulsion, following a first approach of the surfaces.

We have also studied the interactions between mica surfaces bearing adsorbed poly(ethylene oxide) (PEO) layers in an aqueous 0.1 M KNO_3 salt solution,[10,13] a moderately good solvent for the polymer. These showed that, once the limiting adsorption of polymer onto the surfaces had occurred, there was a long-ranged monotonically increasing repulsion between the adsorbed layers ($F(D) > 0$) and also that $F(D)$ depended on the *rate* of compression and decompression of the surfaces; in general $F(D)$ for a given D was found to be lower for the more rapid compression/decompression cycles. The repulsion in this system was largely attributed to osmotic interac-

† Present address: Department of Chemical Engineering and Chemical Technology, Imperial College, Prince Consort Road, London, U.K.
‡ Present address: Polymer Department, Weizmann Institute, Rehovot, Israel.

0024-9297/85/2218-0721$01.50/0

Table I
Molecular Characteristics of the Polymer Samples

	M_w	M_w/M_n	R_g, nm
PEO310	310 000	1.05	18.0
PEO160	160 000	1.04	13.0
PEO40	40 000	1.03	6.5
polystyrene	600 000	1.06	21.0

tions between overlapping segments in the good solvent medium as the quasi-irreversibly adsorbed PEO layers were brought into proximity.

Recently, we investigated the effect on surface–surface forces of *partial* adsorbance of polymer on the surfaces[13]: we found that even in the PEO/0.1 M KNO_3 (good solvent) system there was an initial *attraction* when the surfaces were partly covered by polymer; this changed to an ultimate long-range repulsion (as previously observed[10]) as limiting adsorbance of polymer was attained. This attraction at low coverage was attributed to bridging effects.

The present paper describes an investigation of surface forces between mica sheets in solutions of PEO and of PS in *toluene*, a good solvent for both polymers. It is an extension of our earlier work on PEO in aqueous media[10] to the case of a good (rather than only moderately good) solvent system; the use of a nonpolar organic solvent also eliminates any complications which might be associated with PEO in aqueous electrolytes (such as the possibility of specific structure in these systems[16]) and facilitates interpretation of our results.

Experimental Section

Materials. Toluene was BDH analytical grade material and distilled prior to use. All water (used in cleaning) was freshly double distilled from a fused-silica–glass apparatus. Glassware was cleaned by immersion in K_2CrO_4–H_2SO_4 for several hours and rinsed with water and filtered ethanol (BDH analytical grade) before every experiment.

The mica was Best Quality ruby, muscovite (Kenya), grade 2 FS/GS, supplied by Mica and Micanite Ltd. (U.K.).

The poly(ethylene oxide) used was obtained from Toyo Soda Co. Ltd. (Japan) and was prepared via an anionic polymerization route and terminated with methanol. The polystyrene (Pressure Chemicals Co.) was also anionically polymerized. The molecular characteristics of the polymers used (Table I) were determined by GPC and light scattering (manufacturers' data).

Techniques and Procedure. The apparatus and general procedure for measuring forces $F(D)$ between curved mica sheets immersed in solution a distance D apart have been described in detail previously[8,9] and only deviations specific to the present study will be included. We note especially the use of a small fused-silica bath (volume 25 mL) to enclose the mica surfaces.[11] We recall that the experimental method is capable of measuring (i) D to ±0.3 nm and $F(D)$ to ±50 nN in the range 0–500 nm, (ii) the mean refractive index $n(D)$ of the medium separating the surfaces, (iii) the mean radius of curvature R ($\simeq$1 cm) of the surfaces about the region of closest approach between them.

$F(D)$ between the mica surfaces was first measured in pure toluene. The surfaces were then taken ~2 mm apart and polymer solution was introduced into the cell to the required concentration (100 μg mL^{-1} unless otherwise stated); following introduction of polymer the surfaces were left to incubate overnight (16 ± 2 h) in the solution, and $F(D)$ was again measured. In some experiments the polymer solution was diluted ~1000-fold by two successive exchanges of solution by pure toluene, and $F(D)$ was redetermined for these very dilute polymer concentrations. All solvents and solutions were filtered (Fluoropore, 0.22 μm) prior to introduction into the cell. Cycles of decreasing D (compression) and increasing D (decompression) were carried out at different rates, the time for each cycle ($5 \leq D \leq 300$ nm) varying between ~10 min and 1 h, and force–distance profiles were measured for the various cycles. The interval between cycles varied from ~1 min to several hours, over a total time for an experiment of 1–3 days. Temperatures were monitored via a thermometer placed near the apparatus and were in the range 21 ± 3 °C throughout. All results reported are based on at least three independent experiments (either different pairs of mica sheets or different contact positions for a given pair of sheets).

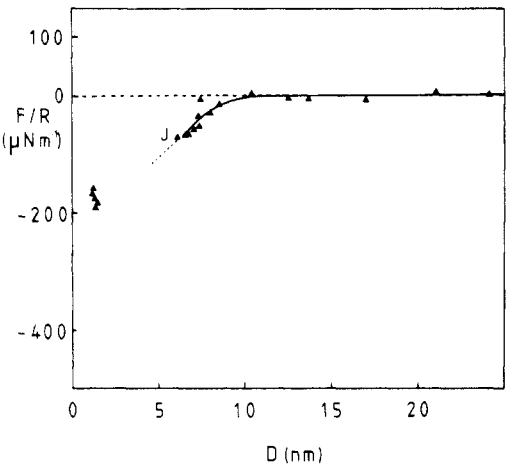

Figure 1. Force–distance profile between curved mica surfaces in pure toluene, where the force axis is normalized as F/R (R is the mean radius of curvature of the mica) to yield the interaction energy per unit area between flat plates, in the Derjaguin approximation[17] (see also text). J indicates an inward jump due to mechanical instability.

Results

Before addition of polymer in any experiment the $F(D)$ profile between the bare mica surfaces immersed in toluene was first determined. Figure 1 shows a typical profile for this case. The force axis is normalized as F/R, where R is the mean radius of curvature of the curved mica sheets in their mutual cross-cylinder configuration; in the Derjaguin approximation[17] (nearly exact for $R \gg D$ as in the present experiments) this gives the interaction energy per unit area $E(D)$ of flat parallel surfaces a distance D apart obeying the same force–distance law as

$$F/R = 2\pi E(D)$$

This normalization is used in all subsequent force–distance profiles. No forces were detected as the surface approached from large D (~300 nm) down to $D \leq 10$ nm, where an attraction was observed; on further compression the surfaces jumped spontaneously from $D \simeq 7 \pm 1$ nm to a new position about 1 nm out from the air contact position, as shown in Figure 1. Such jumps are due to mechanical instability and are expected whenever $\partial F(D)/\partial D \geq K$, the spring constant of the leaf spring supporting the lower mica surface.

Poly(ethylene oxide) (PEO). The following force–distance profiles are for PEO of various molar masses adsorbed onto the mica sheets; we focus also on the effect on $F(D)$ of the different rates of the compression–decompression cycles.

Figure 2 shows the force profiles determined after introducing PEO310 (M = 310 000) into the cell (to a concentration 100 ± 5 μg mL^{-1} in the toluene) and allowing the mica surfaces to incubate in the solution at a separation of 2 mm for 16 h. The results are presented on a log–linear plot to enable the presentation of several orders of magnitude variation in $F(D)$. The salient features of these profiles are characteristic of PEO in toluene and were observed in varying degrees for the other molar mass polymers studied.

On a first approach, following incubation, no interaction was measurable from large D, down to $D \sim 135$ nm (see

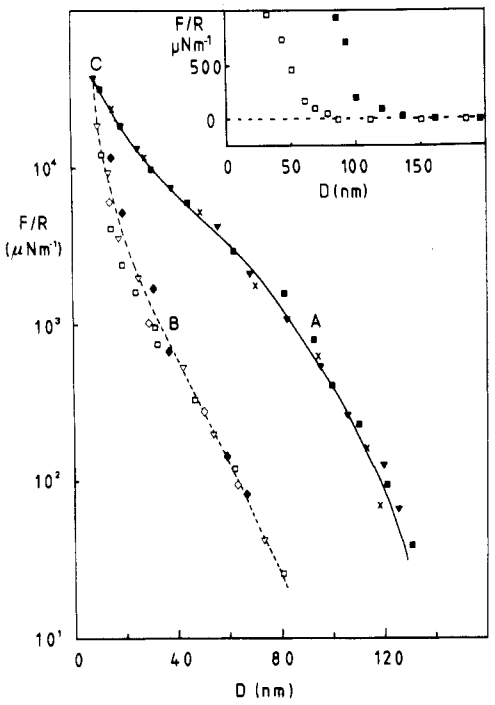

Figure 2. Force-distance profile (normalized as in Figure 1) following 16-h incubation of the mica surfaces in a 100 μg mL^{-1} solution of PEO310 (M = 310 000) in toluene. Solid line A and broken line B refer in general to "relaxed" and "unrelaxed" profiles (see text). (■) First compression following incubation; (□) rapid decompression (following (■)); (♦) second compression (immediately following decompression (□)); (◇) rapid decompression (following (♦)); (▼) third compression (1 h after decompression (◇)); (▽) rapid decompression (following (▼)); (×) compression after replacing PEO310 solution with pure toluene and incubating for 16 h. Inset: F/R vs. D on a *linear* scale for compression–decompression corresponding to symbols (■)/(□) above.

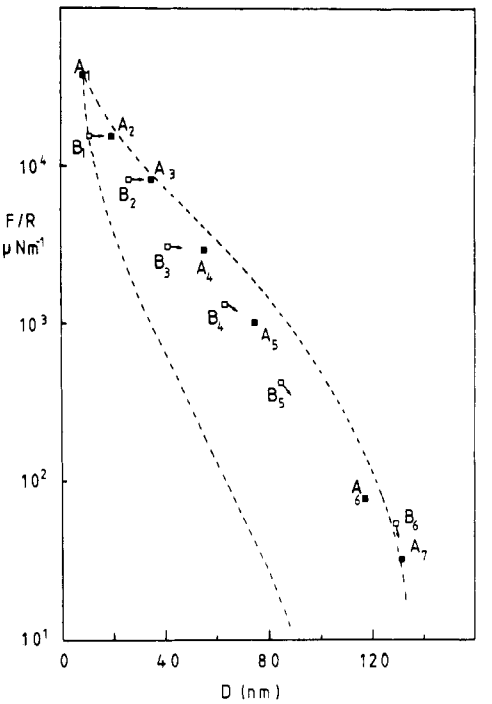

Figure 3. Force–distance profile for same conditions as in Figure 2 for multistage slow decompression. Surfaces taken from A_n to B_n, then left for 15 min, whereon they relax spontaneously (→) to the position A_{n+1}, and so on. Further details in text.

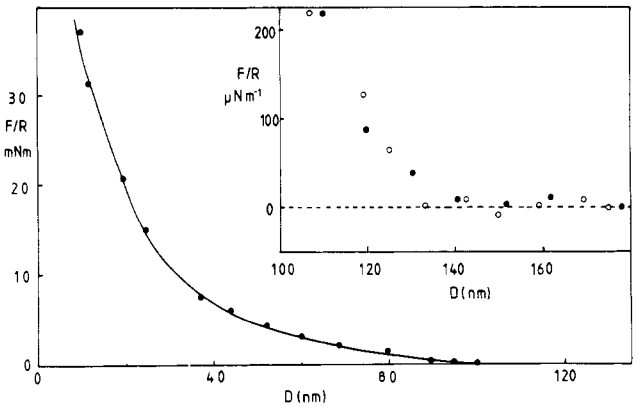

Figure 4. F/R vs. D profile on linear scale following overnight incubation in PEO310 solution in same conditions as in legend to Figure 2. Results for a first compression following incubation are shown. Inset shows results on an expanded scale about the region F = 0 for first compressions for two different experiments, (●) and (○). (i.e., different pairs of mica sheets).

also the inset on Figure 2 showing $F(D)$ vs. D on a linear scale), when a monotonically increasing repulsion was observed down to the point C, at $D \sim 6$ nm, curve A. (This limit was determined by the upper limit of $F(D)$ measurable using the present apparatus.) The behavior on separating the surfaces was dependent upon the rate at which the experiment was performed. For a rapid decompression, i.e., 5–8 min for D going 6 → ~200 nm (the minimum time required to make the measurements), $F(D)$ follows a different profile (broken curve B), becoming indistinguishable from zero (within error) at about D = 80 nm. If the surfaces are recompressed immediately following the rapid decompression (within ~1 min), the resulting $F(D)$ profile was again close to curve B. If, on the other hand, longer periods (≥1 h) were allowed to elapse following the rapid decompression, the subsequent profile on recompression closely followed curve A, as on initial compression following incubation. For intermediate waiting periods (say 10 min following the rapid decompression) the $F(D)$ profile was in the region between curves A and B.

For sufficiently *slow* decompression, however, the resulting force–distance profile was again close to curve A. To investigate this "relaxation effect" more systematically, a slow decompression in stages was carried out as in Figure 3 (for the same polymer, PEO310, and conditions as in Figure 2). The surfaces were withdrawn from point A_n (where A_1 in Figure 3, the point where decompression of the surfaces begins, corresponds to point C in Figure 2) to point B_n, where the force was measured; the system was left for 15 min, while the surfaces moved out spontaneously to A_{n+1}, where $F(D)$ was again determined, then once again the surfaces were withdrawn to B_{n+1}, and so on. Figure 3 shows how the points A_n quite closely follow curve A in Figure 2, while points B_n fall in the region between curves A and B in Figure 2. We note that due to the length of time involved in this slow decompression, cumulative absolute errors, due to random thermal drift of the surfaces, of up to ~200 μN m^{-1} may be present by the end of the decompression half-cycle. The error *between* any two points, however, will be smaller. Figure 4 shows the data corresponding to curve A in Figure 2 on a linear–linear scale (the inset shows the initial stages of interaction on an expanded linear scale). The main feature to note is the absence, within error, of any attractive, or adhesive, component in the interaction.

Figures 5 and 6 summarize the $F(D)$ profiles following incubation of the mica surfaces in 100 μg mL^{-1} PEO160 (M = 160 000) and PEO40 (M = 40 000). The basic features are similar to those obtained for PEO310 presented in Figure 2, in particular the quasi-equilibrium force profiles A (following "relaxation" of the adsorbed layers) and the unrelaxed profiles B, in all systems. The com-

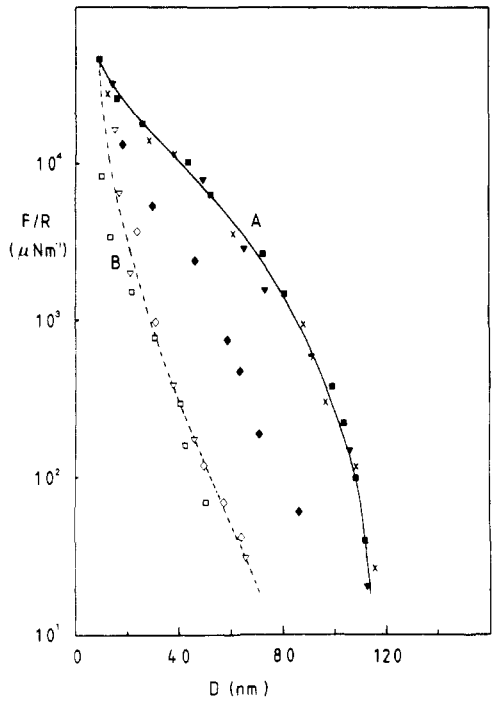

Figure 5. F/R vs. D profiles following overnight incubation (16 ± 2 h) in 100 μg mL^{-1} PEO160 (M = 160 000) in toluene. Solid line A and broken line B refer to "relaxed" and "unrelaxed" profiles (see text). The symbols refer to compression–decompression cycles exactly corresponding to those in Figure 2.

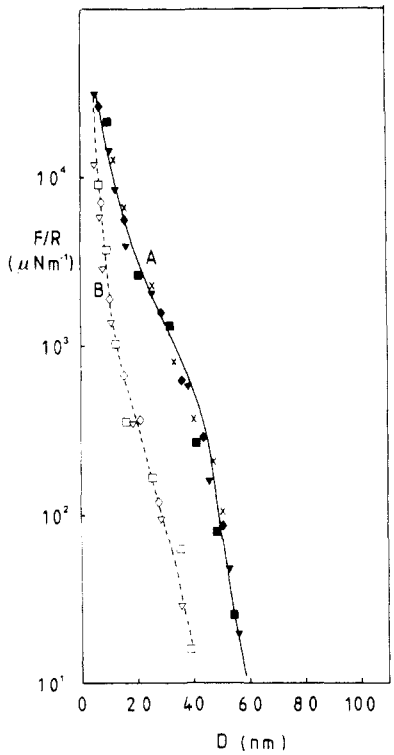

Figure 6. Force–distance profiles following overnight incubation (16 ± 2 h) in 100 μg mL^{-1} PEO40 (M = 40 000) in toluene. Lines A and B refer to "relaxed" and "unrelaxed" profiles (see also text). The symbols refer to compression–decompression cycles exactly corresponding to those in Figure 2.

pression–decompression conditions under which profiles A and B (Figures 5 and 6) were obtained are similar to those of PEO310 (Figure 2), save that when the surfaces are rapidly separated (curves B, Figures 5 and 6) and then rapidly recompressed, the resulting force profiles do *not* follow curve B; rather, they are longer ranged, being intermediate between curves A and B for PEO160 and close to curve A for PEO40. The other main difference is the range at which the repulsive interactions are first detected, 110 and 60 nm for PEO160 and PEO40, respectively (compared with 135 nm for PEO310), indicating a lower extension from the surface of the adsorbed layers of the shorter polymers.

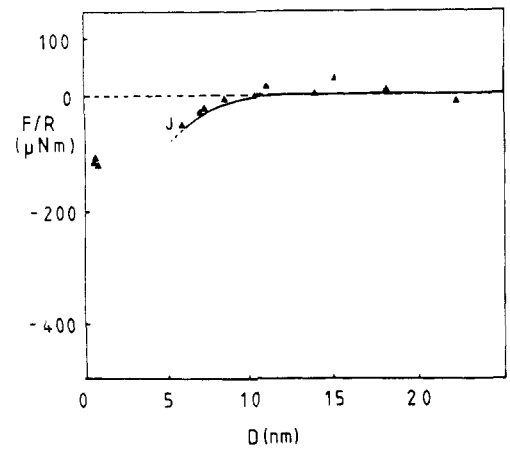

Figure 7. Force–distance profile between two curved mica sheets following overnight incubation (16 ± 2 h) in a 100 μg mL^{-1} solution of polystyrene PS1 (M = 600 000) in toluene.

In several of the experiments (at all molar masses) the PEO solutions were diluted ~1000-fold, by exchange with pure toluene as noted earlier. This extreme dilution did not lead to significant changes in the $F(D)$ profiles (see Figures 2, 5, and 6), indicating little if any desorption as a result of the solution/solvent exchange.

Measurements of the refractive index $n(D)$ following adsorption of the polymer showed little variation with D, as expected, since the refractive index of PEO (1.51) is close to that of toluene (1.49). Unlike previous studies, therefore, it was not possible in the present case to estimate the adsorbance from the $n(D)$ profile.

Polystyrene (PS). Figure 7 shows the force–distance profile between the mica surfaces following overnight (16 ± 2 h) immersion in a 100 μg mL^{-1} solution of polystyrene ($M = 6 \times 10^5$) in toluene. The profile is very similar to that measured between the surfaces in the absence of any polymer (Figure 1) and shows only a short-range attraction ($D \leq 10$ nm) and a jump—as in pure toluene—to an equilibrium position at $D \simeq 1$ nm relative to the air contact position. Similar results were obtained at higher polymer concentrations (up to 0.1% or about 1 mg mL^{-1}) and for polystyrenes of higher molar mass (up to $M = 3 \times 10^6$). Measurements of $n(D)$ showed no significant deviation from the pure toluene case as a function of D, following incubation in the PS solution (we recall that for pure PS, $n_{PS} \simeq 1.6$). Both these observations are consistent with the absence of any adsorbed PS on the mica in the presence of toluene.

Discussion

The short-range attraction between the bare mica surfaces in pure toluene resembles a van der Waals-like interaction (with an appropriate Hamaker constant; see Figure 1) and is closely similar to interaction profiles between mica sheets in cyclohexane and in cyclopentane in previous studies.[9,14,15] We have observed no evidence of structural forces in this system, as reported for other organic solvents (though not toluene; see, e.g., ref 14); the reasons for this, which may be due to "water-bridging" effects[30] and may be associated with the fact that our toluene was not especially dried prior to measurements,

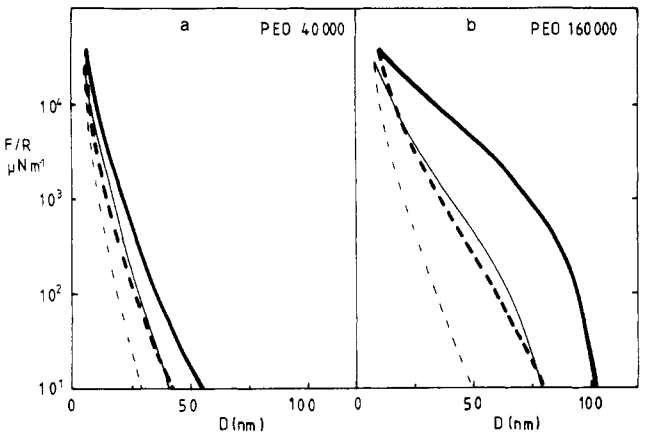

Figure 8. Smoothed interaction–distance profiles between mica surfaces bearing PEO40 (a) and PEO160 (b) in toluene (thick line and thick broken line) (this work) and in 0.1 M aqueous KNO_3 solution (thin line and thin broken line) (ref 10b). The solid and broken curves refer to "relaxed" and "unrelaxed" profiles in the respective solvents (corresponding to curves A and B in Figures 2, 5, and 6, for example).

have been considered previously.[9] We note, however, that the effective "contact" position into which the surfaces jump is at a separation of approximately 1 nm relative to the air contact position (unlike the earlier investigations where the surfaces jumped into the air contact position within experimental error), which may be due to a residual monolayer of toluene molecules adsorbed onto each mica surface. (This point has been considered in detail in the context of other organic solvents.[30]) Toluene has a greater affinity for mica than, say, cyclohexane, as evident from the fact that polystyrene will absorb onto mica from the latter solvent but not from the former. The essential point, however, is that the range over which interactions (whatever their origin) between the *bare* mica surfaces play a significant role, $0 < D \leq 8$ nm, is in general outside the range of interest once PEO had adsorbed (6 nm $\leq D \leq$ 150 nm). This considerably simplifies interpretation of the force–distance profiles in the presence of an adsorbed polymer layer.

We consider first the case of interactions in the PEO/toluene solutions. The main features, at all molar masses of polymer, are (i) long-range, monotonically repulsive, quasi-equilibrium force–distance laws, once overnight adsorption of PEO had occurred (curves A, Figures 2, 5, and 6), and (ii) effects due to *rapid* compression or decompression of the adsorbed layers, which in general lead to lower $F(D)$, for a given D, relative to the slow or quasi-equilibrium force profiles (curves B, Figures 2, 5, and 6).

These features are qualitatively very similar to those observed for interactions between adsorbed PEO layers across 0.1 M KNO_3 aqueous electrolyte[10]; this is shown (in Figure 8) by comparison of the data for PEO160 and PEO40 for the two solvents. The distance for the onset of interactions (curves A in Figures 2, 5, and 6), which is 135, 110, and 60 nm for PEO310, PEO160, and PEO40, respectively, corresponds approximately to $(8.5 \pm 1)R_g$ for the respective polymers (see Table I), where R_g is the unperturbed radius of gyration in each case. Since this distance is typically twice the extension of each adsorbed layer from the surface, the effective layer thickness δ (as detected by our measurements) is thus some $4R_g$ for each polymer. This compares with values for δ of about $3R_g$, observed for PEO160 and PEO40 adsorbed onto mica from 0.1 M KNO_3 in the earlier study (also Figure 8); it also compares well with effective adsorbed layer thicknesses in other polymer/substrate/good-solvent systems, measured by light scattering,[18] ellipsometric,[19] and viscometric[20] techniques.

The origin of the somewhat greater effective extension of adsorbed PEO in toluene ($\delta \simeq 4R_g$) could be partly due to a thicker or more swollen adsorbed layer in the organic solvent, which is a better solvent for the poly(ethylene oxide) than is the aqueous electrolyte (polymer–solvent interaction parameters χ are 0.39 and 0.48 for PEO/toluene[21] and PEO/0.1 M KNO_3[22], respectively). In addition, for a given experimental sensitivity in detecting repulsion between the surfaces, the lower value of χ for PEO in the organic solvent implies that a repulsion would be detected at lower overlap concentration (between opposing adsorbed segments) and hence at a higher D value (see also later discussion).

As noted in the Results, the similarity of refractive indices of pure PEO and pure toluene prevents an estimate of the polymer adsorbance Γ from $n(D)$ in the present case (but see later). The fact that the form of the $F(D)$ curves remains unchanged on ~1000-fold dilution of the solution does however indicate an essentialy irreversible adsorbance of the PEO onto the mica; furthermore, the reversibility of the $F(D)$ curves on (slow) compression–decompression suggests little polymer comes away from the surface on squeezing the adsorbed layers together. This irreversibility has important implications when we come to compare our results with theoretical models.

We observed no attraction (within error, e.g., inset to Figure 4) in the present study, such as could arise from depletion forces[23] (see later) or bridging effects.[1] Attraction due to a given polymer molecule adsorbing simultaneously on both surfaces has in fact been recently observed[13] in the PEO/0.1 M KNO_3/mica system, but only for very low adsorbance of the polymer; the attraction disappeared following full adsorption. In the present study full adsorption of PEO was attained *prior* to any force measurements, and the contribution of attractive bridging forces is therefore swamped by the much greater osmotic repulsion due to interaction between segments in the gap in the quasi-equilibrium force profiles; bridging may, however, partially account for the lower forces observed on rapid decompression of the surfaces (curves B, Figures 2, 5, and 6).

The repulsive forces between the mica plates as they approach are due to osmotic interactions between the segments from opposing adsorbed layers as they come into overlap. The present study is sufficiently direct to permit comparison of the results with predictions of various theoretical models of interactions between polymer-bearing plates. The crucial observation is that the polymer adsorption is essentially irreversible, as has been discussed; this implies that equilibrium models for steric interactions, in which desorption is permitted, may not be appropriate.[23,24] A treatment which can take into account the irreversibility of the adsorption has recently been developed by de Gennes,[24] who has provided calculations for the good-solvent case, and has been extended by Klein and Pincus to the case of poor solvents.[25] In this model the total interaction energy $E(D)$ between two plates bearing adsorbed polymer is minimized with respect to the segment density profile $\phi(z)$, where ϕ is a volume fraction and z is the distance from each plate. The central assumption of this approach is that, for a fixed adsorbance Γ, the values of $\phi(z)$, and in particular $\phi_s = \phi(0)$ (the segment density at the adsorbing surface), adopt their equilibrium values at all surface separations D. Under these conditions, de Gennes has predicted[24] a monotonically increasing repulsion with decreasing separation as the surfaces ap-

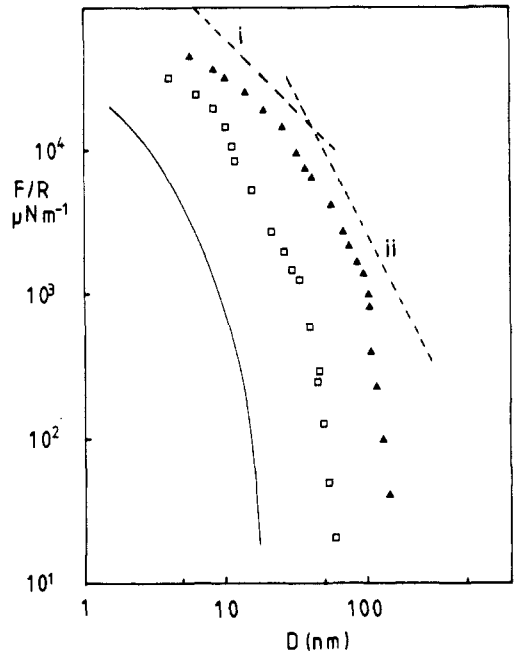

Figure 9. Quasi-equilibrium interaction profiles for mica sheets bearing adsorbed PEO40 (□) and PEO310 (▲) in toluene on a double-logarithmic plot (taken from curves A in figures 2 and 6). The straight broken lines indicate slopes of −1 and −2, respectively, corresponding to (i) $E(D) \propto D^{-1}$ and (ii) $E(D) \propto D^{-2}$, respectively, where $E(D) \equiv (F/2\pi R)$ in the Derjaguin approximation. The solid curve is a plot on the same scale, but with the D axis shifted for clarity, of the interaction between adsorbed layers of PEO160 in aqueous 0.1 M KNO_3 (taken from ref 10b).

proach and overlap of the adsorbed layers occurs. More specifically, the model predicts for good solvents that on initial overlap ($D \leq 2\delta$)

$$E(D) \propto D^{-2}$$

while, on strongly compressing the surfaces

$$E(D) \propto D^{-1.25}$$

Plotted in Figure 9 are F/R ($\equiv 2\pi E(D)$) vs. D profiles for PEO310 and PEO40 on a double-logarithmic scale (taken from the quasi-equilibrium force–distance measurements of Figures 2 and 5). Also shown are the slopes corresponding to the predicted $E(D)$ vs. D variation (broken lines). The solid curve is the profile for PEO160, with the D axis displaced for clarity, from ref 10. We see at once that on initial overlap $E(D)$ varies considerably more rapidly with D than the predicted inverse square law, though over a considerable range of D an inverse square variation fits the data well. Closer in the dependence of $E(D)$ on D is considerably weaker; in any event the scaling exponents used by de Gennes in calculating this (proximal) variation probably do not hold at the high segment densities encountered in the strongly compressed layers. (In this case one expects $E(D) \propto D^{-1}$, as is readily shown.[10b] See also broken line i in Figure 9).

The explanation of the rapid $E(D)$ vs. D variation on initial overlap has been considered in our discussion of the force profiles in the PEO/0.1 M KNO_3 system;[10] it arises because in these initial stages the assumption that $\phi(z)$ and especially $\phi_s = \phi(0)$ responds rapidly to changes in D and in $E(D)$—crucial to the de Gennes model[24]—is not valid. We briefly repeat the argument, assuming now that $\phi(z)$ is *quasi-static* (i.e., does not vary as D decreases) as the adsorbed layers come into overlap. For $D < 2\delta$ (δ is the mean thickness of each adsorbed layer) the *volume* of overlap of opposing layers per unit area (of flat plates, to which our measured $E(D)$ applies) is given by

$$v_0 = 2\delta - D$$

The mean concentration of polymer in the distal region (i.e., the tail) of each adsorbed layer—and hence in the overlap region—is typically exponentially decaying;[23-25] i.e.

$$\phi(D/2) \propto \exp(-\alpha D/2)$$

where α is an inverse correlation length. The osmotic pressure in the overlap region is given by (ignoring scaling exponents and assuming a semidilute concentration)

$$\Pi_0 \propto \nu\phi^2(D/2) \sim e^{-\alpha D}$$

where ν is a virial coefficient (typically $\nu \sim {}^1/_2 - \chi$ in a good solvent), and we have used the semidilute approximation for Π_0.[26,27] The excess energy per unit area of surfaces induced by bringing the adsorbed layers into overlap is then

$$E(D) = v_0\Pi_0 \sim (2\delta - D)e^{-\alpha D}$$

whose logarithm varies with D as

$$\Delta \equiv \frac{\partial(\log E(D))}{\partial(\log D)} = -\frac{D}{2\delta - D} - \alpha D$$

i.e., Δ is large and negative on initial overlap ($D \leq 2\delta$), which agrees with the trend shown in Figure 9. The main physical conclusion suggested by this agreement is that on *initial* (weak) overlap the segment concentration profile probably does not have time (even in our rather slow measurements) to adjust to changes in D. A more detailed discussion is given in ref 10b.

Also shown schematically in Figure 9 is the $E(D)$ vs. D profile for the PEO1/0.1 M KNO_3 system (with the D axis displaced for clarity) and we see again the similarity in the form of the surface–surface interaction between adsorbed layers both in aqueous and organic media. As noted in the Introduction, it has been suggested that PEO in free aqueous solution displays anomalous behavior due to specific structure effects;[16] the similarity in force profiles shown in Figures 8 and 9 strongly indicates that, with respect to steric interaction, the behavior in the 0.1 M KNO_3 medium does not differ from the more "ideal" organic medium of the present investigation.

The effect on $F(D)$—or $E(D)$—of rapid decompression can also be qualitatively understood in terms of a quasi-static segment density distribution. Following compression, ϕ_s attains some high value; on rapid decompression of the surfaces, ϕ_s remains higher than its equilibrium value—for a certain relaxation time—and in consequence the mean segment density of polymer in the surface–surface gap remains momentarily *lower* than its equilibrium value. As a result the mean osmotic pressure in the gap, and hence $F(D)$, is temporarily lower but relaxes to its higher equilibrium value with time. This relaxation trend is clearly seen in Figure 3 and, more generally, in the difference between the rapid (B curves) and slow (A curves) force–distance profiles.

Although we cannot obtain a measure of the adsorbance of Γ from refractive index variation, we may try to estimate Γ directly from the force–distance profiles. We proceed as follows: in the highly compressed region, $D \leq 30$ nm (Figure 9 for PEO310, for example), we assume that the surface concentration of adsorbed polymer has reached a limiting value (for example, if all surface sites are occupied) and that the polymer in the gap is uniformly distributed at a uniform volume fraction ϕ. Any variation in D would then result in a new value for ϕ given by

$$\phi = \phi(D) \approx 2\Gamma\bar{v}/D \qquad (1)$$

where $\bar{v}$ is the partial specific volume for the polymer and Γ is the amount of polymer adsorbed irreversibly per unit area per surface. The pressure between the plates is then equal to the osmotic pressure in the gap,[24] $\Pi(\phi(D))$; if the surface separation changes from D_1 to D_2, the change in surface energy is given approximately by

$$\Delta E = E(D_2) - E(D_1) \approx \int_{D_1}^{D_2} \Pi(\phi(D))\, dD \qquad (2)$$

For the functional form of $\Pi(\phi)$ in terms of ϕ (and hence D) we may use the full Flory–Huggins expression[26]

$$\Pi(\phi) = -\frac{RT}{v_1}\{\ln(1-\phi) + \phi + \chi\phi^2\} \qquad (3)$$

where v_1 is the molar volume of the solvent (toluene), which is a good approximation at the high polymer concentrations in the gap at high compression. From the values for PFO310 (Figure 9) at $D \leq 30$ nm and using literature values for the PEO partial specific volume in toluene and for the toluene–PEO interaction parameter χ, we estimate (using eq 1–3) an adsorbance $\Gamma_{PEO310} \simeq 2$ mg m^{-2} on each mica surface. A similar analysis of the data for PEO40 (Figure 9) yields $\Gamma_{PEO40} \simeq {}^1/_2\Gamma_{PEO310} \simeq 1$ mg m^{-2} per mica surface. This is lower than the adsorbance estimated from refractive index measurements in the PEO/mica/0.1 M KNO_3 system, and it will be of interest to compare these estimates with more direct determinations of Γ, for example using a microbalance approach as developed recently by Terashima.[28]

Polystyrene (PS). The results for the interaction between mica surfaces following incubation in polystyrene solution are very different from the PEO results and indicate that no polymer is adsorbed onto the mica. In previous studies there have already been indications that PS is only weakly adsorbed onto mica: thus in cyclohexane some of the polymer appears to desorb as the solvent conditions are improved by heating from 23 °C ($T < \Theta$) to $T \geq \Theta$;[14] in addition, the adsorbance of PS onto mica in cyclopentane[15] at room temperature ($T \geq \Theta$) is lower than in cyclohexane in poor-solvent[9] conditions, and furthermore, partial *desorption* of the PS occurs when the solution (of polystyrene in cyclopentane) is diluted.[15] The present results, where no adsorption at all of the PS takes place in a *good* solvent, are consistent with these indications.

In the present experiments the *solvent (toluene)–substrate* interaction is the same for both the PEO and PS solutions; in addition, the *solvent–polymer* interaction is similar for the two polymers (with $\chi \simeq 0.40$ in both cases). Thus the reason why PEO adsorbs onto mica from toluene, while PS does not, is almost certainly associated with the *polymer–substrate* interaction energies, which must be higher for PEO than for polystyrene. This may be due to a weak specific chemical interaction between PEO and mica, possibly through the ether oxygen in PEO.

Our measurements represent the first direct investigation of forces between nonadsorbing surfaces in a polymer solution, where "depletion layer" forces might be expected; *it is appropriate, in view of the "null result" obtained* (compare Figures 1 and 7), to examine more closely the conditions under which such depletion layer attraction might be observed in experiments of this type. We recall the origin of depletion layer attraction: when two nonadsorbing surfaces in a dilute polymer solution are within a separation $D < R_g$ of each other, it becomes entropically unfavorable for free polymer molecules to enter the gap between them. As a result the gap becomes largely depleted of polymer, and the osmotic pressure within the gap is lower than in the bulk solution: this "negative pressure difference" results in attraction between the surfaces. The above qualitative argument applies to a dilute (nonoverlapping) polymer solution; for an overlapping (semidilute) concentration ($\phi > \phi^*$, the overlap volume fraction of polymer), the extent of the depletion layer is the *correlation length* ξ (the "mesh" size of the polymer network) as suggested both by scaling arguments[27] and by studies of permeation of polymer into micropores.[29] Thus for $\phi > \phi^*$, we expect depletion layer attraction at $D \leq \xi$.

While there are detailed models[23] for the depletion interaction, we may estimate its magnitude crudely as follows: for a pair of parallel plates a distance D apart, in equilibrium with a free polymer solution of volume fraction ϕ, the interaction energy per unit area $E(D)$ may be written as

$$E(D) = \int_{\infty}^{D} \Delta\Pi\, dx$$

where $\Delta\Pi$ is the osmotic pressure difference between the free solution and the interplate gap. (We ignore any field-type interactions such as van der Waals or electrostatic forces.) In line with our expectation of polymer exclusion from the gap for $D \leq \xi$, we approximate

$$\Delta\Pi \simeq 0, \qquad D > \xi$$

$$\Delta E \simeq \Pi(\phi), \qquad D < \xi$$

where $\Pi(\phi)$ is the osmotic pressure in the free solution, so that

$$E(D) \simeq -(\xi - D)\Pi(\phi) \qquad \text{for } D < \xi$$

$$E(D) \simeq 0 \qquad \text{for } D > \xi$$

(recall also $\xi < R_g$ for $\phi \geq \phi^*$ and $\xi = R_g$ for $\phi < \phi^*$).

Can such magnitudes of $E(D)$ be detected with our apparatus? From Figure 1 or 7 we may impose a lower limit on D, D_0 say, the range at which bare mica–mica interactions become important. For the present experiments with PS, at a polymer concentration of 100 μg mL^{-1} corresponding to $\phi \simeq 10^{-4} < \phi^*$, and $\xi = R_g \simeq 20$ nm, we expect the osmotic pressure to be given by the "ideal" (dilute limit) term

$$\Pi(\phi) = kT(\phi/Na^3)$$

where N is the number of monomers and a is a monomer size, so that (ϕ/Na^3) is the number of polymer chains per unit volume. Thus at a separation $D = D' < R_g$ we have

$$E(D') \simeq -(R_g - D')kT(\phi/Na^3)$$

For PS of $M = 6 \times 10^5$ at a concentration 100 μg mL^{-1} and at $D' = 10$ nm, we have (at room temperature)

$$E(D') \simeq 4 \times 10^{-3}\ \mu\text{J m}^{-2}$$

This is 2–3 orders of magnitude smaller than the inherent detection limit of our technique (± 1 μJ m^{-2}). Even at the overlap concentration for this polymer ($\phi^* \simeq 10^{-2}$) the value of $E(D')$ is still lower than our detection limit.

At higher concentration, $\phi > \phi^*$, we have $\xi < R_g$; if we are to avoid the region of "field-type" effects we must also have $D > D_0$; i.e., for depletion attraction to be dominant we must have $D_0 \leq D \leq \xi$. D_0 is about 5–10 nm whether for van der Waals effects, for structural effects, or in an aqueous electrolyte solution at high salt concentration; i.e., we must have $\xi \geq 10$ nm. It is straightforward to show that with these limits on ξ and D (corresponding to a polymer solution of about 3–5% concentration), for polymer in an athermal solvent ($\chi = 0$), at room temperature

$$E(D_0) \simeq O(50\ \mu J\ m^{-2})$$

In obtaining this estimate we have used the semidilute approximation[26] for $\Pi(\phi) \simeq (1/2)(1 - 2\chi)\phi^2 kT/a^3$. For normal good solvents we expect $\chi \simeq 0.3$–0.4, which reduces $\sim$3-fold our estimate for $E(D_0)$.

These somewhat crude estimates suggest the following:

(i) For $\phi \leq \phi^*$ our method is unlikely to pick up the long-range ($D \simeq R_g$) depletion layer effects.

(ii) At concentrations of a few percent of polymer in good solvent, the estimated depletion attraction *may* be detectable with our technique, but only over a limited range $D_0 \leq D \leq \xi$, where $D_0 \simeq 5$–10 nm and ξ is the correlation length.

Finally we note that the above discussion holds for *equilibrium* between the depleted layer and the bulk solution. It is not obvious that this applies, even at the long times of our experimental measurements, when the attainment of such equilibrium is limited by diffusion of polymer between the surface–surface gap and the bulk solution. (See, e.g., appendix to ref 15.) This is because the *lateral* gap dimensions in our experiment are large; attainment of equilibrium would be much more rapid for the case of interaction between submicron-sized colloidal particles.

To conclude: the interactions between mica sheets immersed in toluene are short-ranged ($\leq$10 nm) and attractive, reminiscent of van der Waals-like forces between the surfaces. Following addition of PEO (of different molar masses) to the toluene and overnight incubation, the interaction for slow compression or decompression is reversible, long-ranged ($\sim(8.5 \pm 1)R_g$, the unperturbed radii of gyration of the respective polymers), and monotonically repulsive. For rapid cycles ($\sim$5 min) of compression and decompression the forces (for a given surface separation) are smaller, relaxing to the limiting quasi-equilibrium profiles at longer times. These features closely resemble those observed for interactions between mica surfaces bearing adsorbed PEO in aqueous salt solution (0.1 M KNO_3).

Following addition of polystyrene to the toluene (to concentrations up to 0.1%) and overnight incubation of the surfaces, the interaction does not change within error relative to the polymer-free case. This suggests that little or no adsorption of polystyrene occurs. A consideration of the magnitude of possible "depletion layer" effects indicates that at these solution concentrations any attractive "depletion layer" forces would be beyond the detection limit of our experiment.

Acknowledgment. We thank the SERC for support to one of us (P.F.L.).

Registry No. PEO (SRU), 25322-68-3; polystyrene (homopolymer), 9003-53-6.

References and Notes

(1) "Colloidal Particles: Polymer Adsorption and Steric Stabilization"; Goddard, E. D., Vincent, B., Eds.; American Chemical Society: Washington, D.C., 1984; ACS Symp. Ser. No. 240.
(2) Faraday Discuss. *Chem. Soc.* **1978**, *65*.
(3) Doroszkowski, A.; Lambourne, R. *J. Colloid Interface Sci.* **1973**, *43*, 97.
(4) Cairns, R. J. R.; Ottewill, R. H.; Osmond, D. W. J.; Wagstaff, I. *J. Colloid Interface Sci.* **1976**, *54*, 45.
(5) Lyklema, J.; van Vliet, T. *Faraday Discuss. Chem. Soc.* **1978**, *65*, 25.
(6) Cain, F. W.; Ottewill, R. H.; Smitham, J. B. *Faraday Discuss. Chem. Soc.* **1978**, *65*, 33.
(7) Tabor, D. *J. Colloid Interface Sci.* **1977**, *58*, 1.
(8) Israelachvili, J. N.; Adams, G. E. *J. Chem. Soc., Faraday Trans. 1* **1978**, *74*, 975.
(9) Klein, J. (a) *Nature (London)* **1980**, *288*, 248; (b) *J. Chem. Soc., Faraday Trans. 1* **1983**, *79*, 99.
(10) Klein, J.; Luckham, P. F. (a) *Nature (London)* **1982**, *300*, 429; (b) *Macromolecules* **1984**, *17*, 1041.
(11) Luckham, P.; Klein, J. *J. Chem. Soc., Faraday Trans. 1*, **1984**, *80*, 865.
(12) Klein, J.; Luckham, P. F.; Almog, Y. In "Colloidal Particles: Polymer Adsorption and Steric Stabilization"; Goddard, E. D., Vincent, B., Eds.; American Chemical Society: Washington, D.C., 1984; ACS Symp. Ser. No. 240, p 227.
(13) Klein, J.; Luckham, P. *Nature (London)* **1984**, *308*, 836.
(14) Israelachvili, J. N.; Tirrel, M.; Klein, J.; Almog, Y. *Macromolecules* **1984**, *17*, 204.
(15) Almog, Y.; Klein, J. *J. Colloid Interface Sci.*, in press.
(16) Edwards, C. J. C.; Rigby, D.; Stepto, R. F. T. *Macromolecules* **1981**, *14*, 1808.
(17) Derjaguin, B. V. *Kolloid-Z.* **1934**, *69*, 155.
(18) Cosgrove, T.; Crowley, T. L.; Vincent, B. In "Adsorption from Solution"; Rochester, C., Ottewill, R. H., Eds.; Academic Press: London, 1983.
(19) Kawaguchi, M.; Hayakawa, K.; Takahashi, A. *Macromolecules* **1983**, *16*, 631.
(20) Priel, Z.; Silberberg, A. *J. Polym. Sci., Polym. Phys. Ed.* **1978**, *16*, 1917.
(21) Ansorena, F. J.; Fernandez-Berridi, M. J.; Barandiaran, M. J.; Guzman, G. M.; Iruin, J. J. *Polym. Bull.* **1981**, *4*, 25.
(22) Vincent, B.; Luckham, P. F.; Waite, F. A. *J. Colloid Interface Sci.* **1980**, *73*, 508.
(23) Scheutjens, J. M. H. M.; Fleer, G. J. *Adv. Colloid Interface Sci.* **1982**, *16*, 341, 360.
(24) de Gennes, P. G. *Macromolecules* **1981**, *14*, 1637; **1982**, *15*, 429.
(25) Klein, J.; Pincus, P. *Macromolecules* **1982**, *15*, 1129.
(26) Flory, P. J. "Principles of Polymer Chemistry"; Cornell University Press: Ithaca, NY, 1953.
(27) de Gennes, P.-G. "Scaling Concepts in Polymer Physics"; Cornell University Press: Ithaca, NY, 1979.
(28) Terashima, H.; Klein, J.; Luckham, P. F. In "Adsorption from Solution"; Rochester, C., Ottewill, R. H., Eds.; Academic Press: London, 1983; p 299.
(29) Cannell, D.; Rondelez, F. *Macromolecules* **1980**, *13*, 1599.
(30) Christensen, H. Thesis, Australian National University, Canberra, 1984.